

# COMPUTATION OF SUPERCRITICAL FLOW IN CHANNEL JUNCTIONS

A Thesis Submitted

In partial Fulfilment of the Requirements

for the Degree of

MASTER OF TECHNOLOGY

by

RAJIV BHARGAVA

to the

DEPARTMENT OF CIVIL ENGINEERING

INDIAN INSTITUTE OF TECHNOLOGY KANPUR

AUGUST, 1991.

CE  
1991  
M  
BHA  
COM

Th  
CE/1991/14  
B.

## CERTIFICATE

It is certified that the work contained in the thesis entitled "*Computation of Supercritical Flow in Channel Junction*", by "*Rajiv Bhargava*", has been carried out under my supervision and that this work has not been submitted elsewhere for a degree.

*B.S. Murty*

15228

( DR. B.S. MURTY )

DEPARTMENT OF CIVIL ENGINEERING  
I.I.T. KANPUR

23 DEC 1991

CENTRAL LIBRARY

Acc. No. A112558

CE-1991-M-BHA-COM

## ACKNOWLEDGEMENT

I am grateful to Dr. B.S.Murty, who is my thesis advisor for his valuable advice, constant inspiration and encouragement during the thesis work.

I am also grateful to Dr.K.Subramanya, Dr. S. Ramaseshan , Dr. Bithin Datta, Dr. V.Lakshminaryana, Dr. B.P.Singh for their valuable guidance during the course work.

I am thankful to my friends specially Jaikumar,Sandeep, Yashkant, Gopal Krishna Mishra, Akshay for their continuous help during my thesis work. My special thanks to Mr. R.C.Srivastava for drawing very nice figure.

Finally I am thankful to all those who have helped me directly or indirectly during the thesis work.

**RAJIV BHARGAVA**

# CONTENTS

LIST OF SYMBOLS	vi	
LIST OF FIGURES	viii	
LIST OF TABLES	x	
ABSTRACT		
CHAPTER- 1	INTRODUCTION	1
1.1	Experimental and analytical studies on supercritical flows	2
1.2	Analytical approach for maximum water level in channel junctions	6
1.3	Numerical modeling of supercritical flows	11
1.4	Present study	14
CHAPTER- 2	GOVERNING EQUATION	15
2.1	Shallow water equation	17
2.2	Assumptions	19
2.2.1	Hydrostatic pressure distribution.	20
2.2.2	Depth averaging and turbulent effect.	21
2.3	Coordinate transformation.	23
CHAPTER- 3	NUMERICAL SCHEME	28
3.1	MacCormack scheme	31
3.2	Initial and boundary conditions.	33
3.2.1	Flow boundaries.	34
3.2.2	Solid side wall boundary	35
3.3	Stability condition.	39

3.4	Artificial viscosity.	40
3.5	Closure	42
CHAPTER- 4	RESULTS AND DISCUSSION	44
4.1	Comparison for 2-D water surface profile	45
4.2	Prediction of maximum flow depth	51
4.3	The numerical sensitivity	60
CHAPTER- 5	SUMMARY AND RECOMMENDATIONS FOR FURTHER INVESTIGATIONS	64
REFERENCES		68

## LIST OF SYMBOLS

$C_n$  = Courant number;

$g$  = acceleration due to gravity;

$h$  = flow depth;

$x$  = space coordinate;

$y$  = space coordinate;

$i$  = subscript for space node in  $\zeta$  direction;

$j$  = subscript for space node in  $\eta$  direction;

$k$  = subscript for time level

$S_{ox}$  = channel bottom slope in the  $x$  direction;

$S_{oy}$  = channel bottom slope in the  $y$  direction;

$S_{fx}$  = friction slope in the  $x$  direction;

$S_{fy}$  = friction slope in the  $y$  direction;

$t$  = time;

$\Delta t$  = time interval;

$u$  = flow velocity in the  $x$  direction;

$v$  = flow velocity in the  $y$  direction;

$V$  = magnitude of the resultant velocity;

$\zeta$  = transformed space coordinate;

$\eta$  = transformed space coordinate;

$\Delta\zeta$  = distance increment in  $\zeta$  direction;

$\Delta\eta$  = distance increment in  $\eta$  direction;

$\psi$  = dissipation coefficient;

- $\delta$  = confluence angle;
- $\alpha_x$  = angle between bottom of channel and the x direction;
- $\alpha_y$  = angle between bottom of channel and the y direction;
- u = when used as subscript denotes values for the straight branch upstream of junction;
- l = when used as subscript, denotes values for the angular branch upstream of junction;



## LIST OF FIGURES

Fig.1.1	Supercritical flow in a channel junction.	6
Fig.1.2	Supercritical flow past a wall deflection.	8
Fig.2.1	Plan view of channel.	16
Fig.2.2	Sections of channel junction	16
Fig.2.3	Finite-Difference grid superposed on channel	23
Fig.2.4	A second method of arranging grid.	24
Fig.2.5(a)	Physical plane	25
Fig.2.5(b)	Computational plane	25
Fig.2.5(c)	Final grid	25
Fig.3.1	Finite-Difference grid.	30
Fig.3.2	Finite-difference grid with imaginary points.	36
Fig.3.3	Illustration of boundary grid.	37
Fig.4.1	Plan view of experimental arrangement	44
Fig.4.2	Water surface profile for Run 1	46
Fig.4.3	Water surface profile for Run 2	47
Fig.4.4	Water surface profile for Run 3	48
Fig.4.5(a)	Water level contour for Run 1 (Computed).	49
Fig.4.5(b)	Water level contour for Run 1 (Measured)	49
Fig.4.6(a)	Water level contour for Run 2 (Computed).	50
Fig.4.6(b)	Water level contour for Run 2 (Measured).	50
Fig.4.7(a)	Water level contour for Run 3 (Computed).	51
Fig.4.7(b)	Water level contour for Run 3 (Measured).	51

Fig.4.8	Comparison of Analytical and Numerical result (maximum flow depth $\delta = 22.5^\circ$ ).	57
Fig.4.9	Comparison of Analytical and Numerical result (maximum flow depth $\delta = 45^\circ$ ).	58
Fig.4.10	Comparison of Experimental and Numerical result (maximum flow depth $\delta = 22.5^\circ$ ).	59
Fig.4.11	Comparison of Experimental and Numerical result (maximum flow depth $\delta = 45^\circ$ ).	60
Fig.4.12	Difference in numerical and Analytical results. ( $\delta = 22.5^\circ$ )	61
Fig.4.13	Three-dimensional velocity field for Run2	63
Fig.4.14	Effect of Courant number.	66
Fig.4.15	Effect of variation Dissipation coeff.	67

## LIST OF TABLES

	#
Table 4.1 Experimental details of the three selected runs	52
Table 4.2 Values of $h_u$ , $h_l$ , $F_u$ , $F_l$ , $h_a$ , $h_n$ , $h_e$ , for $\delta = 22.5^\circ$	55
Table 4.3 Values of $h_u$ , $h_l$ , $F_u$ , $F_l$ , $h_a$ , $h_n$ , $h_e$ , for $\delta = 45^\circ$	56

## CHAPTER 1

### INTRODUCTION

In many hydraulic engineering applications, it is required to design open channels for supercritical flow conditions. Spillway chutes sewer systems and outlet works are some common examples where the flow is supercritical. Supercritical flow is also encountered in road drainage works. Some times an increase in the capacity of hydel power plants requires higher velocities of water in the conveying structure and this makes flow supercritical. These high velocity flows can also occur in natural channels. The flow in steep mountainous streams and in rivers could be supercritical during periods of high flows. A typical example of this is dam break flow.

The analysis of supercritical flow is more complicated than the analysis of subcritical flow because of a number of reasons. Roll waves or slug flow may be present due to instabilities which develop when the Froude number is greater than a critical value. Supercritical flows are also accompanied by air entrainment and cavitation. The most important characteristic of supercritical flows is the presence of standing waves and large surface disturbances. Many times it is necessary to provide lateral change of the boundary

confining the flow at supercritical velocities. These local changes either in cross section, slope or wall direction of the channel results in the formation of standing waves which will cross and recross the channel affecting the down stream flow significantly. Supercritical flow through channel junctions is a good example of the above phenomenon. cross-waves similar to those as in contractions develop and pertain a long distance downstream of the channel. Depending on the junction geometry and inflow Froude numbers a hydraulic jump may form in one of the branches. The side walls have to be considerably higher than those normally provided because the maximum height of the free surface may be 10 to 20 times as large as the in flowing depths. Difficulties are encountered at junctions in tunnel spillways or closed channels due to pulsations, air entrainment, transitions to pressurized flow and moving hydraulic jumps, if the height of the downstream channel is insufficient. The present study is an attempt to develop a mathematical model for the analysis of supercritical flows in channel junctions.

### **1.1 Experimental and Analytical studies on supercritical flows**

The first contribution on the subject of supercritical flow in non prismatic channels originated from investigations in the field of gas dynamics. Raibouchinsky and Prandtl were the

first ones to point out the analogy between supersonic flow of air and supercritical flow of water for two dimensional motion (Ippen 1953). Prandtl (1952) developed a graphical method for the analysis of supersonic flow in gases. Preiswerk (1940) extended this method which is based on the characteristics theory to supercritical flow problems in open channels. Laitone (1952) critically examined the concept of hydraulic analogy and illustrated some of its limitations. Loh (1959) has correctly pointed out that the hydraulic analogy is based on the assumption of flows with negligible vertical accelerations, and this is not valid when the shocks are strong. The limitation of the analogy arises from the fact that for gases, Euler equations are more or less exact mathematical representation of the physical phenomenon, but for open channel flows, the shallow water equations, in certain circumstances, are a somewhat crude approximation. However, the experiments conducted by Ippen and Harleman (1950, 1956) indicated that the hydraulic theory based on gas dynamics analogy works well for a wide range of Froude numbers. They concluded that the limitation comes from the fact that no information can be obtained about short waves, rollers and development lengths using the gas dynamics analogy. Engelund and Munch-Petersen (1953) used potential flow theory to show that the expression for the angular position of a small

stationary wave as derived using the gas dynamics analogy is true for an infinitely wide channel. It is actually a function of Froude number and the width to depth ratio.

An excellent summary of the early work on supercritical flows is presented in the "proceedings of a symposium on high velocity flow" (Ippen et al. 1951). Ippen and Knapp (1936, 1938) and Knapp (1951) studied the supercritical flow in the bends. Ippen and Dawson (1951), Harrison (1966) and Sturm (1985) gave design considerations for supercritical flow in contraction. Rouse (1938) and Rouse et al (1951) analyzed supercritical expansions and developed a special geometry for expansions in order to prevent flow separation and to obtain a water profile with minimum of surface disturbances.

Most of the available work on supercritical flows is concerned with the analysis for channel transitions and bends. Very little work has been reported regarding the supercritical flow characteristics in channel junctions. Bowers (1950) seems to be the first to have analyzed supercritical flow through channel junctions. He found that the formation of a hydraulic jump in one of the branches depends on the junction geometry and the inflow Froude numbers. Schnitter et al (1955) conducted experiments in channel junctions where the angle of confluence is almost zero, but the lateral channel had a steep slope. They observed considerable cross wave pattern in the

downstream branch. This wave became strong when the two upstream branches have different in flowing Froude numbers. They also gave guide lines for reducing the perturbations. Behlke and Pritchett(1966) analyzed supercritical flow in junctions for different angles of confluence and for a range of Froude numbers. They presented a theoretical approach for determining wave angles in simple junctions based on relationships established by Ippen and Knapp(1936). This led to identification of wall pile up zones. Greated (1968) also presented similar relationships for the main wave angle at a simple junction. Gerodetti (1978) conducted experiments on supercritical flows as encountered in road drainage channels. He used two semi-circular channels of top width 15 cm, bottom slope of 28%, and an angle of confluence  $\delta=37^{\circ}$ . Recently Hager (1989) used both theoretical and experimental approaches to analyze the main flow features in junctions with thoroughly supercritical flows. The junction is characterized by rectangular channels of equal branch width and sharp edge corners. Junctions angles of  $22.5^{\circ}$  and  $45^{\circ}$  are considered. Their analytical approach, although elegant unfortunately has an error. The correct derivation of equations for estimating maximum height of water level in channel junction based on Hager's approach is presented later. Problem of interest in open channel flows is the division of flow into branch



### 1.2 Analytical approach for maximum water level in channel junctions.

The analytical model given below closely follows the derivation presented by Hager(1989). Unfortunately has an error. This is corrected in the present analysis. Derivation is for "simple junction" that is, a junction where the two inflow branches have a common invert elevation and there are no baffles or piers to deflect the flows at the junction. Also the main channel is straight and is of constant width. Streamline curvature effects are not incorporated.

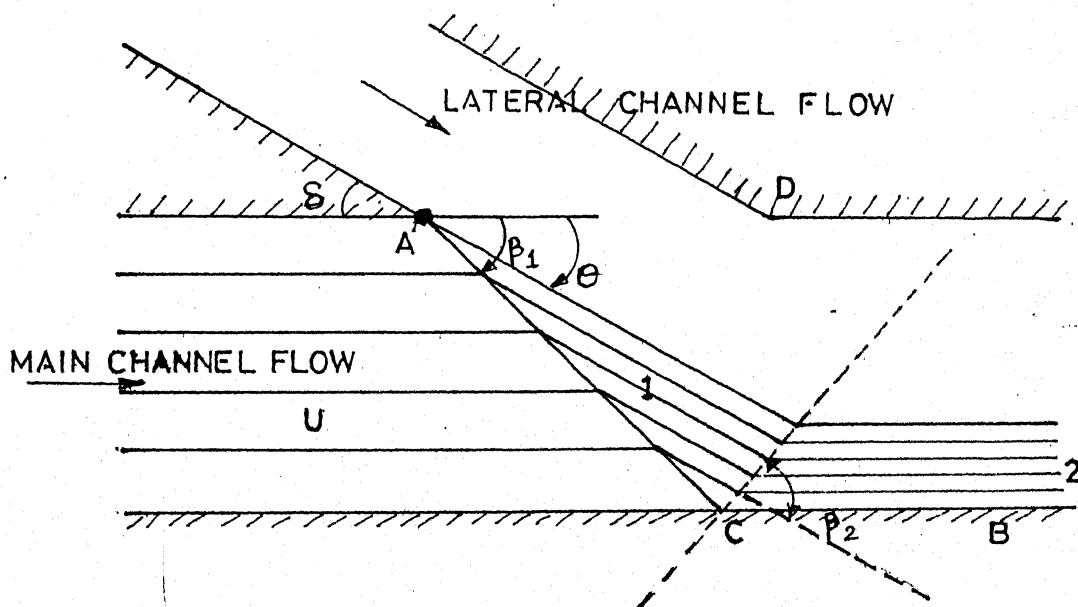


Fig. 1.1

SUPERCritical FLOW IN A CHANNEL JUNCTION

Referring to Fig.1.1, Upstream of point A, two plane flows are present which are characterized by  $h_u, F_u$  and  $h_l, F_l$   $h$ =flow depth,  $F$ =froude number and subscripts  $u$  and  $l$  refer to the values in the main and lateral channels upstream of the junction respectively. At point A, the two undisturbed flows intercept each other, thereby creating a main wave front at an angle  $\theta$  relative to the main direction. The two incoming flows are thus deflected by the angle  $\theta$  (U/s branch) and  $(\delta - \theta)$  (lateral branch) thereby forming two new wave fronts. Due to main wave front at an angle  $\theta$  the upstream flow turns once the wave front at an angle  $\beta_1$  is passed and this latter wave front hits the walls. It is reflection leaves at an angle  $\beta_2$  and streamline become parallel to the wall once this second wave front is passed. Thus three different domain of flow may be distinguished as follows

- (1) upstream zone (index "u" )
- (2) Zone between fronts with angles  $\theta$  and  $\beta_1$  (index "1")
- (3) Zone between wall and wave front with the angle

proposed by Ippen and Knapp.(1936) This is illustrated below.

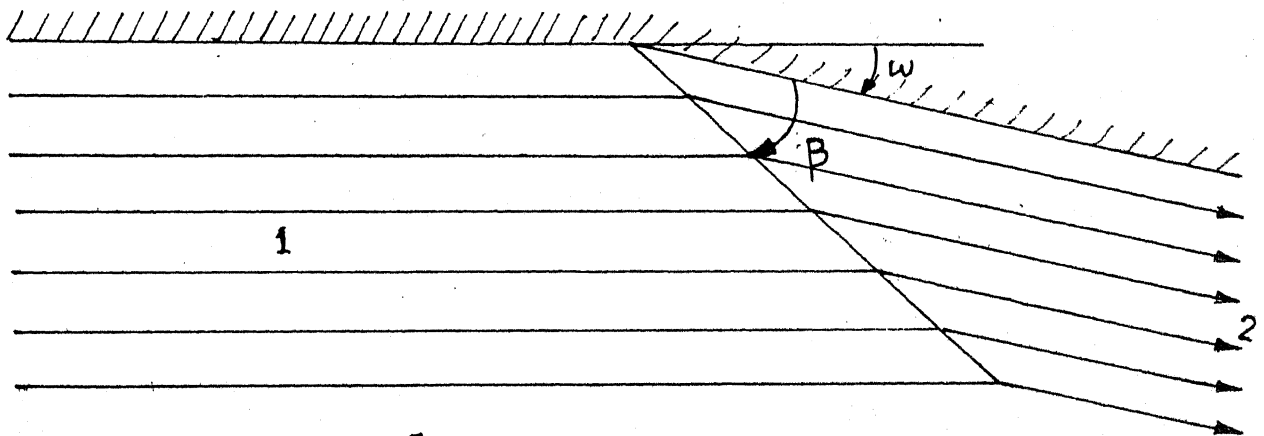


Fig. 1.2  
SUPERCritical FLOW PAST A WALL DEFLECTION

Fig.1.2. show the stream line pattern for supercritical flow past a wall deflection. Here  $\omega$  =the angle by which the wall is deflected i.e. the angle by which the flow changes it directions and is the resultant wave angle. Subscripts 1 and 2 refer to the values upstream and downstream of the wave angle front respectively. The following relationship can be used to determine  $h_2$ ,  $F_2$  and  $\beta$  if  $h_1$ ,  $F_1$ , and  $\omega$  are given.

Fig.1.2. show the stream line pattern for supercritical flow past a wall deflection. Here  $\omega$  =the angle by which the wall is deflected i.e. the angle by which the flow changes its directions and  $\beta$  is the resultant wave angle. Subscripts 1 and 2 refer to the values upstream and downstream of the wave angle front respectively. The following relationship can be used to determine  $h_2$ ,  $F_2$  and  $\beta$  if  $h_1$ ,  $F_1$ , and  $\omega$  are given.

$$h_2/h_1 = 1/2 * [(1 + 8 * F_1^2 * \sin^2 \beta)^{1/2} - 1] \quad \dots\dots\dots(1.1)$$

$$h_2/h_1 = \tan \beta / \tan(\beta - \omega) \quad \dots\dots\dots(1.2)$$

$$F_2^2 = y^{-1} * [F_1^2 - (1/2 * y) * (y-1) * (y+1)^2] \quad \dots\dots\dots(1.3)$$

These three equations constitute the governing system for the determination of the sought quantities  $h_2$ ,  $F_2$ ,  $\beta$  for given  $h_1$ ,  $F_1$  and  $\omega$ . As can be noticed, determination of  $h_2$ ,  $F_2$  and  $\beta$  is implicit Hager and Bretz (1987) derived the following explicit approximate equations from the Eqs.1.1-1.3 for the conditions that  $\beta < 45^\circ$  and  $F_1 > 2$ .

$$h_2/h_1 = \sqrt{2} * F_1 * \sin \beta - 1/2 \quad \dots\dots\dots(1.4)$$

$$\beta = \omega + 3 / (2 \sqrt{2} * F_1) \quad \dots\dots\dots(1.5)$$

$$F_2^2 = F_1 * \cos^2 \beta / (\sqrt{2} * \sin \beta * (1 - 2.0 * f_1)) \quad \dots\dots\dots(1.6)$$

where

$$f_1 = \sqrt{2} * F_1 * \sin \beta \quad \dots\dots\dots(1.7)$$

Applying eqs. 1.4-1.7 to regions "u" and "1" in fig.1.1, We

get

$$\beta_1 = \theta + 3/(2\sqrt{2}Fu) \quad \dots\dots\dots(1.8)$$

$$y_1 = \sqrt{2}Fu \sin \beta_1 - 0.5 \quad \dots\dots\dots(1.9)$$

and

$$F_1^2 = Fu \cos^2 \beta_1 / (\sqrt{2} \sin \beta_1 [1 - (2\sqrt{2} \beta_1 Fu)^{-1}]) \dots\dots\dots(1.10)$$

A similar application for regions 1 and 2 gives

$$\beta_2 = \theta + 3/(2\sqrt{2}F_1) \quad \dots\dots\dots(1.11)$$

$$y_2 = \sqrt{2}F_1 \sin \beta_2 - 0.5 \quad \dots\dots\dots(1.12)$$

and

$$F_2^2 = F_1 \cos^2 \beta_2 / (\sqrt{2} \sin \beta_2 [1 - (2\sqrt{2} \beta_2 F_1)^{-1}]) \dots\dots\dots(1.13)$$

Eqs. 1.8-1.13 can be used to determine  $h_2$  and  $F_2$ . Once the value of  $\theta$ , the angle by which the main flow changes its direction due to interaction with the lateral flow is known,  $\theta$  depends on the inflow parameters  $h_u, h_l, F_u, F_l$  and the confluence angle  $\delta$ . Greated (1968) derived the following equations for simple channel junctions based on the assumptions of uniform velocity and hydrostatic pressure distribution.

$$1 - Y^2 = 2Y^2 Fu^2 \sin^2 \theta - 2f_l^2 \sin^2 (\delta - \theta) \quad \dots\dots\dots(1.14)$$

where

$$Y = h_u/h_l \quad \dots\dots\dots(1.15)$$

Hager (1989) further simplified eq. 1.14 and derived the following.

$$\theta/\delta = [1 + (V_u/V_l)(h_u/h_l)^{1/2}]^{-1} \quad \dots\dots\dots(1.16)$$

Equation 1.16 is valid provided  $\delta \leq 45^\circ$  and

$$1/(|1 - Y^2|)^{1/2} * F1 > 1/\delta$$

In this study Eqs. 1.16 ,1.8 -1.12 are used for determining  $h_2$  for given inflow conditions and the confluence angle.

#### 1.4 Numerical Modelling of Supercritical flows

In spite of the degree of refinement reached in the computation of open channel flows and the significant advances on the subject, it appears that in many aspects the supercritical flows still defy reliable analysis (Lai 1986). Steady two-dimensional shallow water equations constitute a set of hyperbolic partial differential equations. Therefore, characteristic method can be used for their solution. Bagge and Herbich (1967), Herbich and Walsh (1972s), Villagas (1976) and Dakshinamoorthy (1973, 1977) used this method for analyzing steady supercritical flows. Except Dakshinamoorthy (1973), all the above investigators were primarily interested in supercritical flows in channel transitions. Dakshinamoorthy (1973) makes a reference to the problem of flow division in a junction when the upstream flow is supercritical. However, he did not analyze the shock wave pattern in junctions where supercritical flow from one channel interacts with the supercritical flow from another channel. Characteristic method requires many interpolations which could seriously affect the accuracy of the solution. Also , characteristic methods are

not able to compute oblique jumps properly.

The analogy between gas dynamics and shallow water flow has prompted many researchers to borrow techniques developed in the former area and apply them to supercritical flows in open channels. There are two types of techniques to compute flow fields with shocks: "shock-fitting" and "shock-capturing" techniques. Shock-fitting methods treat all shocks as discontinuities and explicitly compute their motion and strength. In shock-capturing techniques, shocks are predicted as part of the solution and need no special treatment. Liggett and Vasudev (1965) are the first to numerically integrate the steady two-dimensional shallow water flow equations. They used the methods developed by Stoker (1957) and analyzed supercritical flow in expansions including the effects of bottom slope and friction. Their method, like the others mentioned above, can not compute flows with shocks or standing jumps. Pandolfi (1975) applied shock-fitting methods for the computation of steady two-dimensional flow around a blunted obstacle in a supercritical flow stream. Demuren (1982) used Patankar and Spalding's method for simulating both subcritical and supercritical flows in open channels. However, the ability of numerical scheme to handle discontinuities is not clearly demonstrated. Recently, Jimenez (1987) and Jimenez and Chaudhry (1988) used a shock capturing technique to

simulate supercritical flow in channel contractions and expansions. Their technique is able to simulate the shock properly. Steady supercritical flow equations are hyperbolic in nature and shock-capturing, marching techniques may be used to simulate the oblique jumps or shocks. It can not be used if the flow is subcritical in part of the channel since the governing equations become elliptic. Therefore, all the methods mentioned earlier are applicable only when the flow is supercritical in the entire length of the channel. In such cases, an unsteady flow model may be used to obtain steady flow solutions by using the false transient method. Such method is capable of simulating mixed sub and supercritical flows if a proper numerical technique is used. In the false transient method, some arbitrary initial conditions are assumed and the boundary conditions are set equal to the initial steady state conditions. Using the governing equations for unsteady flow, the system conditions are computed for sufficient length of time until the variation of flow conditions is negligible and the conditions have converged to steady values corresponding to the boundary conditions. Many numerical schemes are available for solving two dimensional unsteady flows (Katopodes 1984, Garcia and Kahawita 1986, Fennema and Chaudhry 1990). Recently, Bhallamudi and Chaudhry (1991) used this approach for computing steady supercritical



flows in channel expansions and contractions. Their results matched satisfactorily with the results obtained using a steady flow model. The ability of the model to simulate mixed sub and supercritical flows was demonstrated by simulating hydraulic jump in an expansion.

From the above discussion it can be summarized that most of the earlier experimental and analytical work in supercritical flows has dealt with channel transitions and bends. There are some recent works on supercritical flow junctions (Hager 1989). However, analytical methods are based on many assumptions and do not describe the complete two dimensional flow characteristics in channel junctions. Therefore, numerical methods should be used for the analysis. Almost all of the earlier numerical solutions are for channel transitions. To the authors' knowledge, no attempt has been made as of yet to numerically simulate supercritical flow in channel junctions.

### **1.5 Present Study**

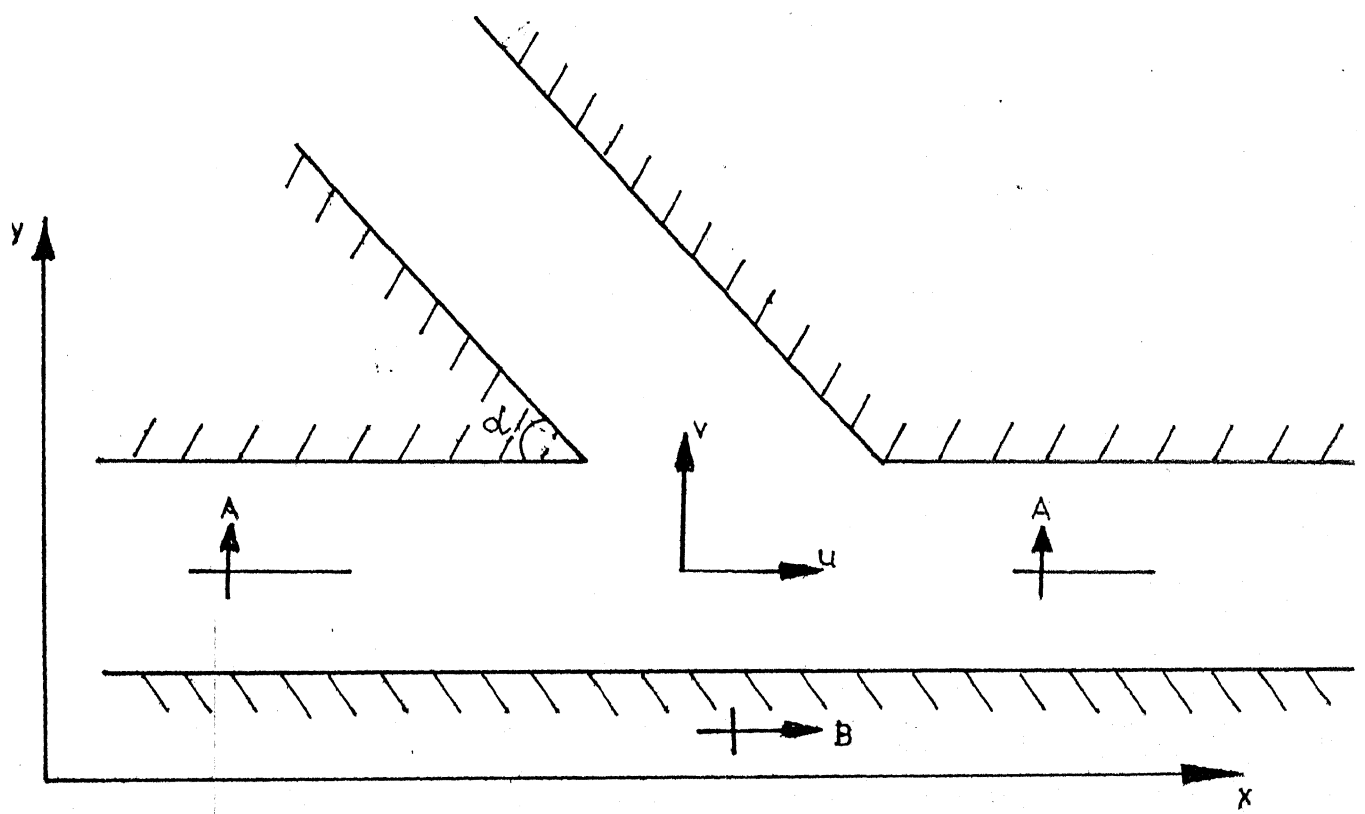
The aim of this study is to develop a mathematical model for the computation of steady two dimensional supercritical flows in channel junctions. It is assumed that the shallow water flow equations describe these flows, although it is recognized that this assumption may restrict the use of mathematical model. Therefore, one objective of this study is

## CHAPTER 2

### GOVERNING EQUATION

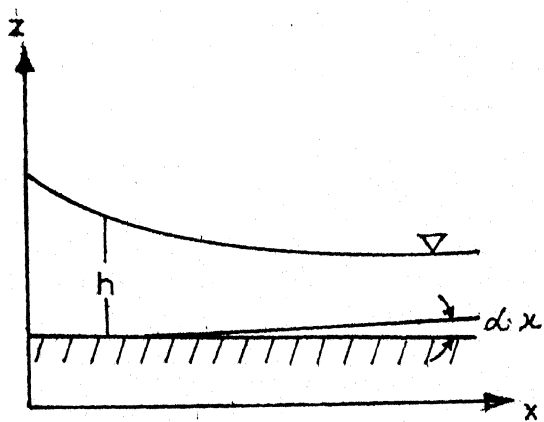
The shallow water equations describe the gradually varied flow in open channels. They follow from the application of the principles of the conservation of mass and momentum. Since supercritical flow in a junction in open channels is characterized by relatively large changes in depth over short distance, shallow water equations are not exactly applicable. However, solution of more general equations describing flows in open channels like Boussinesq type equations which include vertical acceleration effect (neglected in gradually varied flow equation) is not simple even for one-dimensional flows (Gharangik 1988, Abbot et al. 1978). It becomes a lot more complicated for two-dimensional case. Therefore, Shallow water equations are used in this study as a first step towards analyzing supercritical flows in junctions. The limit of applicability is established in an indirect way by comparing numerical results with the experimental data.

In this chapter, the shallow water equations and the assumptions on which they are based are presented. This is followed by the discussion on the limitations of the shallow water theory. The coordinate transformation procedure for transforming the physical plane into a rectangular computational plane is also presented.

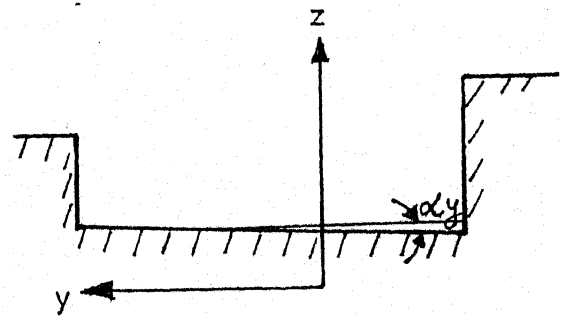


PLAN VIEW

Fig. no. 2.1



SECTION A-A



SECTION B-B

$$S = \begin{bmatrix} 0 \\ -gh(S_{ox} - S_{fx}) \\ -gh(S_{oy} - S_{fy}) \end{bmatrix}$$

Subscripts t, x and y in eq.2.1.indicate the partial derivatives. In the above equation;

t= time

u,v = depth averaged flow velocities in the x,y directions respectively.

h = water depth measured vertically.

g = acceleration due to gravity.

$S_{ox}, S_{oy}$  = Channel bottom slopes along longitudinal and lateral directions respectively.

Channel slopes  $S_{ox}$  and  $S_{oy}$  are given by

$$S_{ox} = \sin \alpha_x \quad \dots\dots\dots(2.2)$$

$$S_{oy} = \sin \alpha_y \quad \dots\dots\dots(2.3)$$

In which

$\alpha_x(x,y), \alpha_y(x,y)$  = angle between the bottom of the channel and the (x,y) direction along longitudinal and lateral direction respectively. (See Fig.2.1)

Friction slopes are estimated using any empirical equation

like Chezy's equation.

$$S_{fx} = (u \sqrt{u^2 + v^2}) / c^2 h \quad \dots\dots\dots(2.4)$$

$$S_{fy} = (v \sqrt{u^2 + v^2}) / c^2 h \quad \dots\dots\dots(2.5)$$

Where

$c$  = Chezy's coefficient.

$S_{fx}, S_{fy}$  = friction slopes in the longitudinal and lateral directions respectively calculated from chezy type equations.

## 2.2 Assumptions

Equation 2.1 is based on the following main assumptions

- 1) The accelerations in the vertical direction are negligible, making the pressure distribution in vertical direction hydrostatic.
- 2). Velocity distribution is uniform along the flow depth.
- 3) The fluid is incompressible and has homogeneous density.
- 4) The channel bottom slope is rigid and small.
- 5) Only shear stresses due to horizontal velocity components are significant, other viscous effects are neglected.
- 6) The frictional resistance is approximated by the chezy or the Manning equations.

A discussion on the fore mentioned assumptions is being

presented in the following paragraphs :

**2.2.1 Hydrostatic pressure distributions** Deviation from hydrostatic pressure distribution is negligible as long as regions of high curvature are not present. Liggett (1975) showed that the above assumption is valid as long as a "shallowness" parameter  $h_0/l_0$  ( $h_0$  = water depth and  $l_0$  = a characteristic length.) is small. However, problem arises in defining the characteristic value in each case. Jimenez(1987) estimated the errors involved in supercritical flow computations if shallow water theory is used. He compared the wave angles obtained using shallow water theory to those obtained using the more rigorous theory of Engelund and Munch-Petersen(1953) based on Potential flow assumption. It was concluded that the shallow water theory reasonably represents the supercritical flow if depth to width ratio is of the order of 0.1 and the Froude number is not close to one. The error is of the order of 20% if the depth to width ratio is increased to 0.2. This error is manifested in the wave length of the resulting wave patterns. Ippen and Harleman (1956) also showed that this theory provides accurate results except in the vicinity of the slope itself . Some details are lost, but the overall results are adequate for engineering purposes (Cunge 1975). One of the main aims in the design of hydraulic structure having supercritical flow is to reduce shocks in water surface profile as much as possible. The

methods based on shallow water equations provide useful results for this purpose.

**2.2.2 Depth averaging and turbulent effect:** The depth integration of the three-dimensional equations of motion produce higher order terms known as effective stresses which are not included in equation 2.1. In a detailed examination of this problem, Flokstra (1977) identified three types of "effective stresses" that arise from the averaging process.

- 1) Laminar viscous stresses

- 2) Turbulent stresses

- 3) Stresses due to depth averaging of advective terms. While the first type of effective stress can be neglected, the other two are important. Consideration of turbulent stresses requires the use of turbulence closure models which express stresses as functions of the mean flow variables. Rastogi and Rodi (1978), Puri and Kao (1984) and Leschziner and Rodi (1979) used "K- $\epsilon$ " models for describing turbulence. Vreugdenhil and Wijkenga (1982) used a much simpler constant eddy viscosity concept. However, the above closure models are tested only for subcritical flows and no information is available for supercritical flows. Non-inclusion of turbulent terms leads to omission of side wall boundary layer effects. Ippen and Harleman (1950) analyzed the case of oblique jump and concluded that reduction

of velocity across the boundary layer reduces the vertical accelerations at the point of wall deflection. This makes the shock front steeper than in the case when the boundary layer is not included.

Ippen and Harleman (1950) studied the effect of non-uniform velocity distribution also. The measurements of velocity across the depth on the front and back side of the jump indicated that the momentum correction factor ranged from 1.007 at  $F = 6.3$  to 1.015 at  $F = 2.0$ . Therefore, they concluded that the effect of velocity distribution may be considered negligible. However, it should be noted that although the effect of magnitude variation of velocity across the depth is not significant, the variation in the direction of resultant velocity may have some effect. This is especially true for flows in channel junctions as found in the experiments by Hager (1989). Fig 4.13 shows the velocity vectors at different depths for supercritical flow in a channel junction. As can be seen, the velocity is almost parallel to the side wall near the channel bottom and it is pointing towards the wall near the surface. Equation 2.1 can not simulate this effect and the numerical results will be in error. As mentioned earlier, one of the purposes of this study is to partially estimate the errors due to above assumptions by comparing numerical results with the experimental data.



Before this discussion is closed, it should be pointed out that it is not possible to simulate separation if the effective stresses are not included (Flokstra 1977). Any circulating pattern in numerical results obtained without the inclusion of the effective stress terms is only an indication of numerical errors. It should also be mentioned that only channels with vertical side walls are considered in the present study. There are several complications in the case of non rectangular channels from a computational point of view because of the existence of zones that become dry or wet and theoretically because the depth may become zero at the edge of the channel.

### 2.3 Coordinate transformation

In this study, a finite-difference method is used to solve eq. 2.1. Physical boundary as well as the finite difference grid in cartesian coordinate system for a channel junction are shown in Fig.2.3.

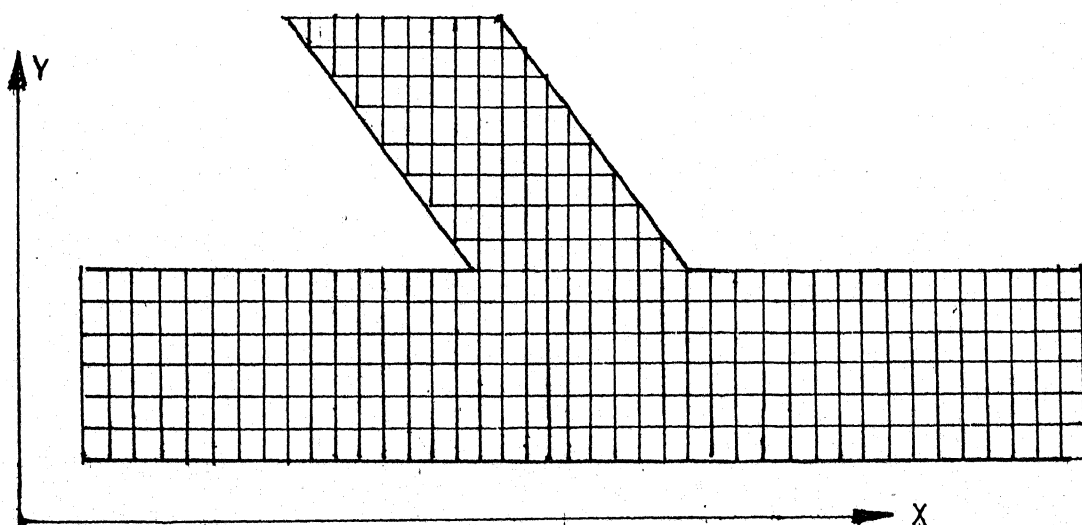


Fig. 2.3

We notice that it becomes necessary to represent the physical boundary in angular portion in a stair step fashion. It leaves sharp corners (marked 1 on Right side and 2 on Left side). Sharp corners introduce numerical disturbances which spread quickly to entire mesh. This may result in numerical instability (Roache 1972). This is particularly so for supercritical flows which are hyperbolic in nature. An alternative method of arranging the grid could be as in Fig.2.4

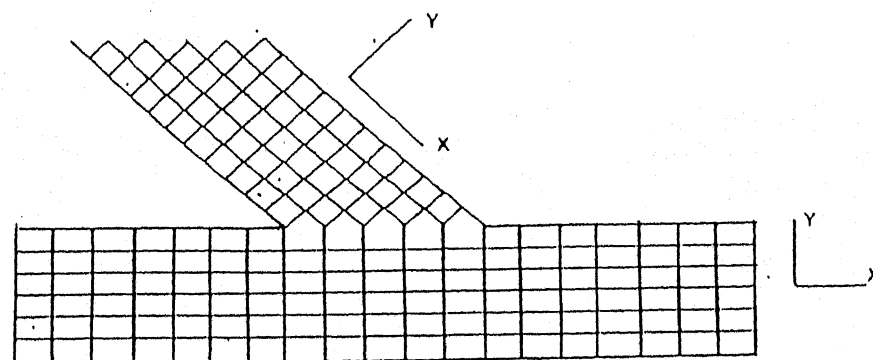


Fig. 2.4

This again leaves wedges at the junctions of two channels and also requires different coordinate directions for straight and angular channels. Aforementioned problems can be avoided by using a coordinate system such that the coordinate axes coincide with the boundaries (Anderson et. al. 1984). Use of a simple algebraic coordinate transformation suffices in the present case.

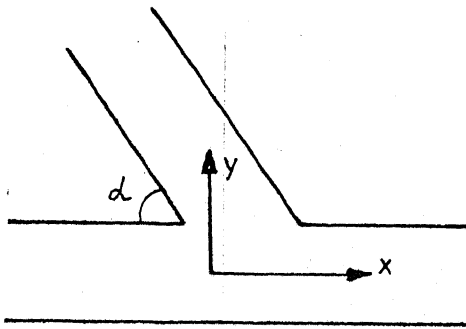
The following transformation of independent variables converts the original physical plane (2.5a) into a rectangular computational plane (Fig 2.5 b.)

$$\zeta = x + y \cot \alpha$$

.....(2.6)

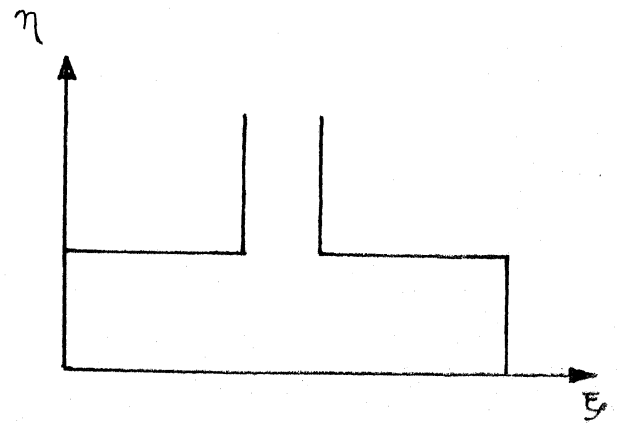
$$\eta = y / \sin \alpha$$

.....(2.7)



PHYSICAL PLANE

Fig. 2.5 (a)



COMPUTATIONAL PLANE

Fig. 2.5(b)

With this, coordinate axes coincide with physical boundaries (See Fig.2.5c)

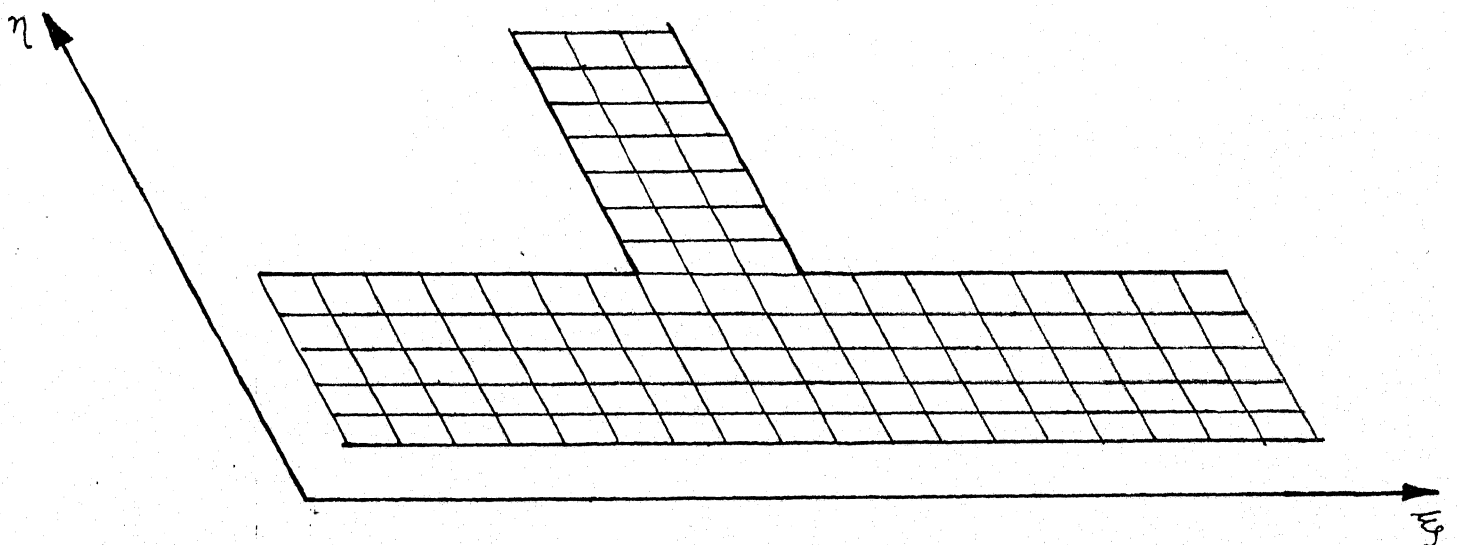


Fig. 2.5 (c)

The governing equations must be expressed in terms of the new independent variables for their application. This is done by applying the chain rule of partial differentiation as follows:

$$\partial/\partial x = (\zeta_x * \partial/\partial \zeta) + (\eta_x * \partial/\partial \eta) \quad \dots\dots\dots(2.8)$$

$$\partial/\partial y = (\zeta_y * \partial/\partial \zeta) + (\eta_y * \partial/\partial \eta) \quad \dots\dots\dots(2.9)$$

Subscripts denote partial derivatives. Eqs. 2.6 and 2.7 give

$$\zeta_x = 1 ; \quad \eta_x = 0 \quad \dots\dots\dots(2.10)$$

$$\zeta_y = \cot \alpha ; \quad \eta_y = 1/\sin \alpha \quad \dots\dots\dots(2.11)$$

$$\partial/\partial x = \partial/\partial \zeta ; \partial/\partial y = \cot \alpha * \partial/\partial \zeta + (1/\sin \alpha) * \partial/\partial \eta \quad \dots\dots\dots(2.12)$$

Application of equation 2.12 to equation 2.1 and subsequent rearrangement of terms yields the following conservation equation.

$$E_t + \bar{F}_x + \bar{G}_y + S = 0 \quad \dots\dots\dots(2.13)$$

In which

$$E = \begin{bmatrix} h \\ hu \\ hv \end{bmatrix}$$

$$\bar{F} = \begin{bmatrix} uh + hv * \cot \alpha \\ u^2 h + gh^2/2 + huv * \cot \alpha \\ uvh + (hv^2 + gh^2/2) \cot \alpha \end{bmatrix}$$

$$\bar{G} = \begin{bmatrix} vh/\sin \alpha \\ uvh/\sin \alpha \\ (v^2 h + gh^2/2)/\sin \alpha \end{bmatrix}$$

$$S = \begin{bmatrix} 0 \\ -gh(S_{ox} - S_{fx}) \\ -gh(S_{oy} - S_{fy}) \end{bmatrix}$$

Equation 2.13 is solved in this study using a finite-difference method. The details of the numerical scheme are presented in the following chapter.

## CHAPTER 3

### NUMERICAL SCHEME

The shallow water flow equations presented in the previous chapter constitute a set of hyperbolic partial differential equations. Analytical solutions for these are available only for highly simplified cases. Therefore, they are usually solved by suitable numerical techniques. Either finite-difference or finite-element techniques can be used for this purpose. Finite element techniques for open channel flows are only in an infancy stage and their application is complicated, especially for flows with shocks such as those considered here. Therefore, a finite-difference method is chosen in this study. We are interested only in the steady supercritical flow characteristics in junctions. These steady flow characteristics are obtained by the false transient method. Any initial conditions, such as constant velocity and a constant depth, through out the system are assumed and the boundary conditions are set equal to the steady-state conditions. Using the two-dimensional unsteady flow equations, the system conditions are computed for sufficient length of time until the variation of flow conditions is negligible and the conditions have converged to the steady values corresponding to the boundary conditions. In other words, the

time is used as an iteration parameter.

The supercritical flow in channel junctions is associated with a complex pattern of shocks. Therefore, it becomes convenient to use a shock capturing technique rather than a characteristic method with shock fitting procedures. According to the theory upon which these methods are based (Lax 1954, Lax and Wendroff 1960, Abbott 1974) three steps should be considered.

- 1) The governing partial differential equations should be in conservation form. Reason for this is that Eq.2.1. expresses the laws of conservation of mass and momentum, and these are the quantities which are actually conserved through a jump.

- 2). The numerical scheme should be conservative. In other words, the scheme should exactly maintain the discretized version of conservation laws for any mesh size and over any arbitrary finite regions.

- 3) The numerical scheme should be dissipative in nature in order to represent the energy losses associated with hydraulic shocks (Roache 1972). This dissipation should be very small in regions of gradual variation, but comparatively large near a discontinuity (Abbot 1975). Some numerical schemes, particularly the first order schemes, have "inbuilt" dissipation mechanism. The schemes which do not have

"inbuilt" dissipation require explicit inclusion of viscosity, known as "artificial viscosity" for successful application.

Shock capturing techniques can not precisely resolve the shock location and they have a tendency to produce spurious oscillations near the strong shocks. The first objection is valid when the shocks are true discontinuities. However, this is not the case in open-channel applications. The spurious oscillation near a shock front originate because the conservative variables being differentiated across the shock may have discontinues derivatives (Kutler 1975). Generally, these oscillations are a characteristic of second and higher order schemes. These oscillations can be reduced by

- 1) introducing artificial viscosity and
- 2) aligning one of the coordinate axes in the direction of shock (Anderson et. al. 1984).

Application of the finite-difference methods require the use of a finite difference grid as shown in Fig. 3.1.

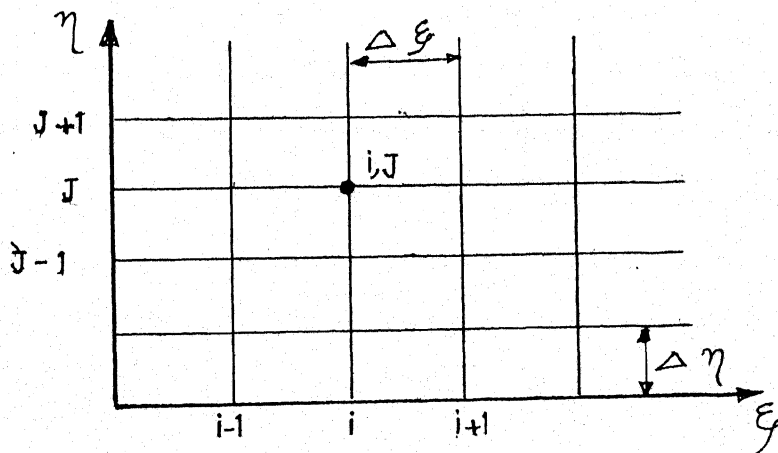


Fig. 3.1



The values of the dependent variables at a grid point are identified by the node  $(i,j)$ .  $i$  indicates the position along  $\xi$  direction and  $j$  indicates the position along  $\eta$  direction.  $\Delta\xi$  and  $\Delta\eta$  are mesh step sizes in the  $\xi$  and  $\eta$  directions respectively. The dependent variable are known at any time either as initial conditions or through computations for a previous time step. The values of the variables after a time step of  $\Delta t$  i.e. at time  $t + \Delta t$  are determined using the finite difference technique as described in the next section.

### 3.1 MacCormack Scheme

A large number of numerical schemes are available to solve hyperbolic system of equations. In general, the choice of a particular method is directed by several factors such as the simplicity of programing, accuracy, efficiency and the particular application under consideration. Besides these considerations accuracy, convergence, diffusive properties, stability etc. of a numerical scheme are also important consideration. MacCommack scheme is used for the problem under study. It is an explicit, second order accurate shock capturing scheme for solving hyperbolic equations. This scheme is explained in detail elsewhere and only a brief description is given here. It comprises of a predictor and a corrector step. In the predictor part, backward finite-differences are used for approximating spatial partial differential terms.

In the corrector part, they are approximated by the forward difference scheme, using predicted values. With reference to the finite-difference grid shown in Fig.3.1 these approximations are

Predictor part

$$\partial f / \partial \xi = (f_k(i,j) - f_k(i-1,j)) / \Delta \xi \quad \dots\dots\dots(3.1)$$

$$\partial f / \partial \eta = (f_k(i,j) - f_k(i,j-1)) / \Delta \eta \quad \dots\dots\dots(3.2)$$

$$\partial f / \partial t = (f_p(i,j) - f_k(i,j)) / \Delta t \quad \dots\dots\dots(3.3)$$

where  $f$  is used for any function of which the partial derivative is required. The subscript  $k$  denotes the value of the function at known time level, i.e. at time  $t$ , subscript  $p$  refers to the values at the end of the predictor step.  $\Delta t$  is the computational time step.

Corrector part

$$\partial f / \partial \xi = (f_p(i+1,j) - f_p(i,j)) / \Delta \xi \quad \dots\dots\dots(3.4)$$

$$\dots \partial f / \partial \eta = (f_p(i,j+1) - f_p(i,j)) / \Delta \eta \quad \dots\dots\dots(3.5)$$

$$\partial f / \partial t = (f_c(i,j) - f_p(i,j)) / \Delta t \quad \dots\dots\dots(3.6)$$

Where subscript  $c$  indicates the value of the function at the end of corrector step. The value of the function at the unknown time level i.e. at time  $t+\Delta t$  is given by the following

$$f_{k+1} = 0.5*(f_k + f_c) \quad \dots\dots\dots(3.7)$$

Substitution of Eqs.3.1 to 3.7 in Eq. 2.1 leads to explicit algebraic expressions for the determination of h, u and v at the unknown time level  $t + \Delta t$  if the values are known at time t. This requires that initial conditions be given for starting the unsteady computations. Once the values are known at  $t + \Delta t$  these are used to determine the values at time  $t + 2\Delta t$ . This marching in time is continued till steady values of h, u and v are obtained.

The above procedure can be used for all nodes  $i=2, \max(i)$  and  $j=2, \max(j)$  where  $\max(i)$  is the last but one node in  $\xi$  direction and  $\max(j)$  is the last but one node in  $\eta$  direction. Boundary Conditions have to be applied at the boundary nodes. Initial and boundary conditions are explained in the next section.

### 3.2 Initial and Boundary Conditions

As mentioned earlier, initial conditions have to be specified in order to start the computation. Since we are using a false transient method to obtain steady state flow characteristics, any initial conditions such as constant velocity and constant depth equal to the boundary value may be assumed for all nodes.

The determination of u, v and h at the boundary nodes

during unsteady computation involves the application of boundary conditions. The treatment of the boundaries is one of the most important aspects in the successful application of any numerical technique (Moretti 1969). Hyperbolic equations are particularly sensitive because errors introduced at the boundaries are propagated and reflected throughout the grid, and in many cases instabilities may result (Anderson et al. 1984). The literature covering the numerical applications to hydraulic problems refers to this subject rather scarcely. Two types of boundaries are encountered in the present study. They are

- 1) Flow boundaries and
- 2) Solid side wall boundaries.

The treatment of the boundaries in the numerical mode is described below.

### **3.2.1 Flow Boundaries**

Stoker (1957), Abbott (1979) and Cunge et al. (1980) discussed the mathematical basis for the specification of open boundaries in shallow water wave applications. Based on the characteristic theory, it can be shown that for two dimensional supercritical flows, three boundary conditions have to be specified at the inflow boundary and none at the out flow boundary.

$u$ ,  $v$  and  $h$  are specified at the inflow sections of main and lateral channels as upstream boundary conditions.  $u$ ,  $v$  and  $h$

at the downstream end are obtained simply by extrapolation from the values at the interior nodes already calculated by MacCormack scheme. Although, this procedure is not exact, the errors introduced are limited to only few nodes at the downstream end. This is because the flow is supercritical and has an upstream control. A disturbance can travel only in the downstream direction and not in the upstream direction.

### 3.2.2 Solid side wall boundary

The basic requirement for a solid boundary is that there is no flow normal to it. This is expressed as

$$\tan\theta = v/u \quad \dots\dots\dots(3.8)$$

where  $\theta$  is the angle between the wall and the axis. This is called the slip condition and is the proper boundary condition at a side wall since all the stresses other than the bottom stress are neglected. For inviscid gas flow applications, several wall boundary techniques have been developed (Abbett 1971, Moretti 1969, Roache 1972, and Anderson et al. 1984). All these techniques try to enforce in one way or another the basic requirements given by eq 3.8. The problem arises because, in order to apply the numerical scheme at the grid points along the wall, the values of all the variables are required and the

equation does not provide enough information. Therefore, it is necessary to find a way to compute these values using information from the interior points plus the boundary condition. The problem was studied by Abbett (1971) who compared and classified them into four broad categories as follows;

- 1) Reflection or image point procedures.
- 2) One sided derivatives procedures.
- 3) Procedures based on the method of characteristics and
- 4) Abbet's procedure.

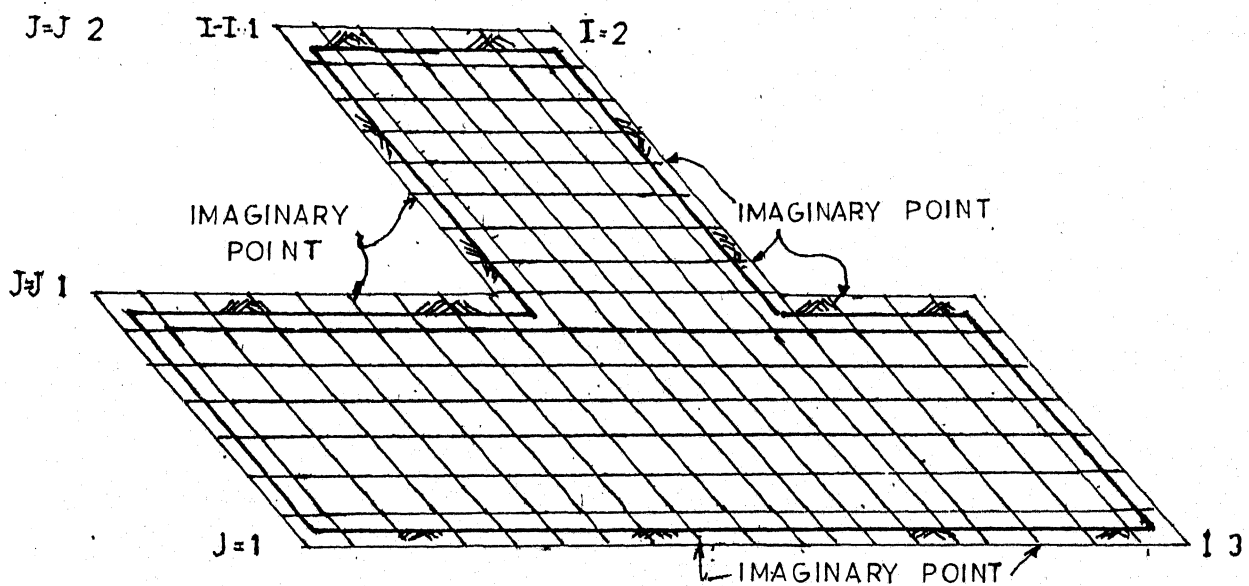


Fig. 3.2

Jimenez (1987) tested several techniques for the case of steady supercritical flow in transitions and concluded that the Abbet's procedure is best suited for this purpose. However, this

procedure is applicable only for steady flow conditions and is not suitable for unsteady flow computation done here. The reflection procedure seems to be more suitable than the other techniques and is used herein. In this procedure, all non-conservative flow variables other than the normal velocity component (i.e.  $u$ , and  $h$ ) are considered even functions with respect to the wall. The normal velocity is assumed an odd function to ensure zero normal velocity at the wall. In implementing reflection, an imaginary row of points is considered as shown in fig. 3.2. values of the variable at the imaginary points are assigned according to the above symmetry conditions. For the purpose of illustration let us consider boundary next to  $J=1$  row (Fig.3.3.)

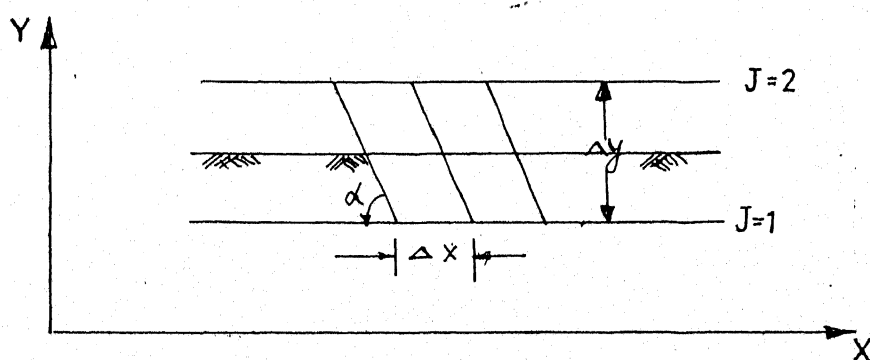


Fig. 3.3

Since wall under consideration is aligned with the X axis, boundary condition is given by  $v = 0$  at the boundary. The

reflection procedure is slightly modified here because of transformations of independent coordinates. The mathematical representation of reflection procedure in cartesian coordinate system is as below.

$$\partial h / \partial y_{\text{wall}} = 0 \quad \dots\dots\dots(3.9)$$

$$\partial u / \partial y_{\text{wall}} = 0 \quad \dots\dots\dots(3.10)$$

$$\partial v / \partial y_{\text{wall}} = (2*v)_{\text{wall}} / \Delta y \quad \dots\dots\dots(3.11)$$

Substitution of Eqs. 2.6.-2.12 in Eqs. 3.9-3.11 results in the following equations which are valid at a solid side wall boundary.

$$\text{Cos}\alpha * \partial h / \partial \zeta + \partial h / \partial \eta = 0 \quad \dots\dots\dots(3.12)$$

$$\text{Cos}\alpha * \partial u / \partial \zeta + \partial u / \partial \eta = 0 \quad \dots\dots\dots(3.13)$$

$$\text{Cos}\alpha * \partial v / \partial \zeta + \partial v / \partial \eta = 2*v / \Delta \eta \quad \dots\dots\dots(3.14)$$

The finite difference approximation of eqs. 3-12-3.14 for the solid side wall shown in Fig 3.3. gives the following explicit equations for determining h, u and v at any node (i,1).

$$h(i,1) = h(i,2) + \Delta \eta / \Delta \zeta * \{h(i+1,2) - h(i,2)\} * \text{Cos}\alpha \quad \dots\dots(3.15)$$

$$u(i,1) = u(i,2) + \Delta \eta / \Delta \zeta * \{u(i+1,2) - u(i,2)\} * \text{Cos}\alpha \quad \dots\dots(3.16)$$

$$v(i,1) = -v(i,2) + \Delta \eta / \Delta \zeta * \{v(i+1,2) - v(i,2)\} * \text{Cos}\alpha \quad \dots\dots(3.15)$$



$h$ ,  $u$  and  $v$  are determined at the interior node  $(i, 2)$  using the MacCormack scheme. These are then used in Eqs. 3.15-3.17 to determine  $h$ ,  $u$  and  $v$  at the boundary nodes  $(i, 1)$ . Similar procedure is used at all other solid side wall boundaries. Reflection procedures are relatively easier to implement. However, they have been criticized because of the introduction of additional conditions at the boundaries (such as Eqs. 3.9 and 3.10) which represent symmetric conditions there by over specifying the problem (Moretti 1969). Roache (1972) examined this problem and showed that if the grid is set as shown in Fig 3.3. (i.e. setting the wall at  $y = 0.5\Delta y$  the errors introduced by the reflection procedure is minimum.

### 3.3 Stability condition

The mathematical foundations for the question of stability of numerical schemes are well developed only for linear systems. The results from linear theory are used as guidelines to nonlinear problems, the justifications depending on numerical experiments. Governing equations for our case are nonlinear.

MacCormack scheme is stable if the courant-Friedrichs-Lewy (C F L ) condition is satisfied at every grid point. This condition for two dimensional flows is heuristically expressed by the following equations (Roache 1972)

$$Cn = \{(V + \sqrt{gh})\Delta t \sqrt{(\Delta \zeta^2 + \Delta \eta^2)}\} / (\Delta \zeta / \Delta \eta) \leq 1 \dots \dots (3.18)$$

In terms of  $\Delta t$

$$\Delta t = Cn / (v + \sqrt{gh}) * (1 / \sqrt{(1/(\Delta \zeta^2) + 1/(\Delta \eta^2))}) \dots \dots (3.19)$$

In which  $V$  is resultant velocity at the grid point and  $Cn$  should be less than one. Above condition is based on a linearized form of the governing equations for one dimensional flows. A certain amount of numerical experimentation is required before choosing the actual upper limit for  $cn$ .

### 3.4 Artificial Viscosity

MacCormack scheme is second order accurate in space and time and results in dispersive errors (Anderson et al 1984). These dispersive errors cause high-frequency oscillations near steep gradients. In the model presented herein, the procedure developed by Jamison et al. (1981) is used to dampen these high frequency oscillations. This procedure smoothens regions of large gradients while having smooth areas relatively undisturbed. The values of the variable at the new time computed by MacComack method are modified using the following algorithm.

$$v_{\zeta} = \frac{|h(i+1,j) - 2*h(i,j) + h(i-1,j)|}{|h(i+1,j)| + |2*h(i,j)| + |h(i-1,j)|} \dots \dots (3.20)$$

$$v_{\eta} = \frac{|h(i, j+1) - 2h(i, j) + h(i, j-1)|}{|h(i, j+1)| + |2h(i, j)| + |h(i, j-1)|} \quad \dots\dots(3.21)$$

At points where  $h(i, j-1)$  does not exist

$$v_{\eta} = \frac{|h(i, j+1) - h(i, j)|}{|h(i, j+1)| + |h(i, j)|} \quad \dots\dots(3.22)$$

At points where  $h(i, j+1)$  does not exist

$$v_{\eta} = \frac{|h(i, j-1) - h(i, j)|}{|h(i, j-1)| + |h(i, j)|} \quad \dots\dots(3.23)$$

At points where  $h(i-1, j)$  does not exist

$$v_{\zeta} = \frac{|h(i+1, j) - h(i, j)|}{|h(i+1, j)| + |h(i, j)|} \quad \dots\dots(3.24)$$

At points where  $h(i+1, j)$  does not exist

$$v_{\zeta} = \frac{|-h(i, j) + h(i-1, j)|}{|h(i, j)| + |h(i-1, j)|} \quad \dots\dots(3.25)$$

$$v_{\zeta(i-\sigma, j)} = K * \max(v_{\zeta(i-1, j)}, v_{\zeta(i, j)}) \quad \dots\dots(3.26)$$

$$v_{\eta(i-\sigma, j)} = K * \max(v_{\eta(i-1, j)}, v_{\eta(i, j)}) \quad \dots\dots(3.27)$$

Where  $K$  is a dissipation constant. The corrected values of the variable  $f$  at the new time step are given by the following equation.

$$f(i,j) = f(i,j) + A + B \quad \dots\dots\dots(3.28)$$

Where  $A$  and  $B$  are

$$A = \{f(i+1,j) - f(i,j)\} * \psi_{\zeta(i+0.5,j)} - \{f(i,j) - f(i-1,j)\} * \psi_{\zeta(i-0.5,j)}$$

$$B = \{f(i+1,j) - f(i,j)\} * \psi_{\eta(i,j+0.5)} - \{f(i,j) - f(i-1,j)\} * \psi_{\eta(i,j-0.5)}$$

Value of variable  $f$  is the one obtained after the corrector step. Dissipative constant,  $K$ , is used to regulate the amount of dissipation. The above procedure is equivalent to adding second order dissipative terms to the original governing equations. The actual numerical eddy viscosity coefficient is of the order of  $K\psi\zeta * (\Delta\zeta^2 / \Delta t^2)$ . This indicated that the influence of  $K$  on the results depends upon gradients in the flow depth as well as grid size. Equations show that influence of this procedure of artificial viscosity is minimal in smooth regions. Since  $\psi$  tends to zero in such a case. Kroll and Jain (1987) showed that the influence of dissipation coefficient is reduced considerably, if the grid is refined and consequently a slightly larger value of  $K$  is needed to smooth out the oscillations. It should be noted here that the presence of friction term which is dissipative in nature tends to inhibit the oscillations. Therefore, a small value of  $K$  is sufficient for smoothing in such situations .

### 3.5 Closure

In this chapter, MacCormack scheme for solving the governing equation has been presented. The boundary conditions, stability criteria and the artificial viscosity procedure have

been discussed. The principles presented here were used to develop a computer program for analyzing the supercritical flow in channel junctions. Results of this study are presented in the following chapter.

## CHAPTER 4

### RESULTS AND DISCUSSION

To verify the mathematical model presented in chapter 2 and 3, computed results are compared with laboratory test data (Hager 1989). The numerical results are also compared with the analytical solution for maximum flow depth (sect.1.3) to determine range of parameters for which the analytical model correctly simulates the two-dimensional flow pattern.

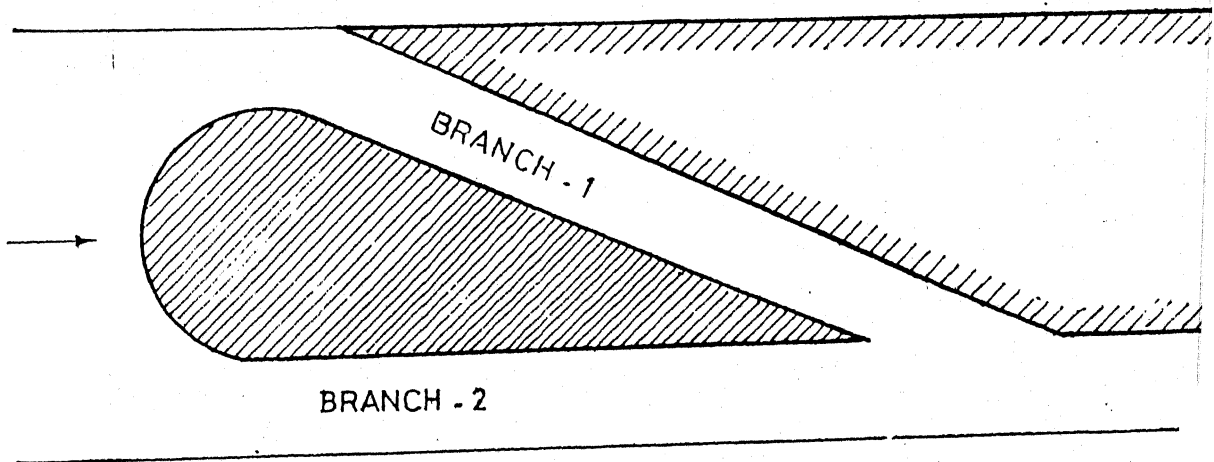


Fig. 4.1 PLAN VIEW OF EXPERIMENTAL ARRANGEMENT.

The experiments (Hager 1989) were performed in a rectangular, horizontal channel 50 cm wide. Two elements were inserted in the channel as shown in the Fig.4.1, making the widths of the three branches equal to 99 mm each. Two junction angles,  $\delta = 22.5^\circ$  and  $45^\circ$  were considered. The flow depths were controlled by two vertical, movable gates which were placed immediately upstream of the junction. The length of the downstream branch was 60 cm and after this it expanded again to the full channel width of 50 cm. The main test section was situated between the gates and the end of the downstream branch. Two types of test were conducted. Flow depths  $h_u$  and  $h_l$ , the velocities  $v_u$  and  $v_l$ , the angle of the main wave front  $\theta$  and the maximum flow depths  $h_{max}$  were measured in majority of the runs. The Froude numbers covered the ranges  $2.8 < F < 16$  for  $\delta = 22.5^\circ$  and  $3.3 < F < 8.3$  for  $\delta = 45^\circ$ . The entire three-dimensional velocity field and the flow surfaces were recorded for three selected runs. These selected runs were made for  $\delta = 22.5^\circ$ . A point gauge ( $\pm 0.1$  mm) and a propeller velocity meter ( $\pm 3$  cm/s) were used to take measurements.

#### 4.1 Comparison For 2-D Water Surface Profile

The inflow conditions for which the entire water surface profile was measured are given in Table 4.1

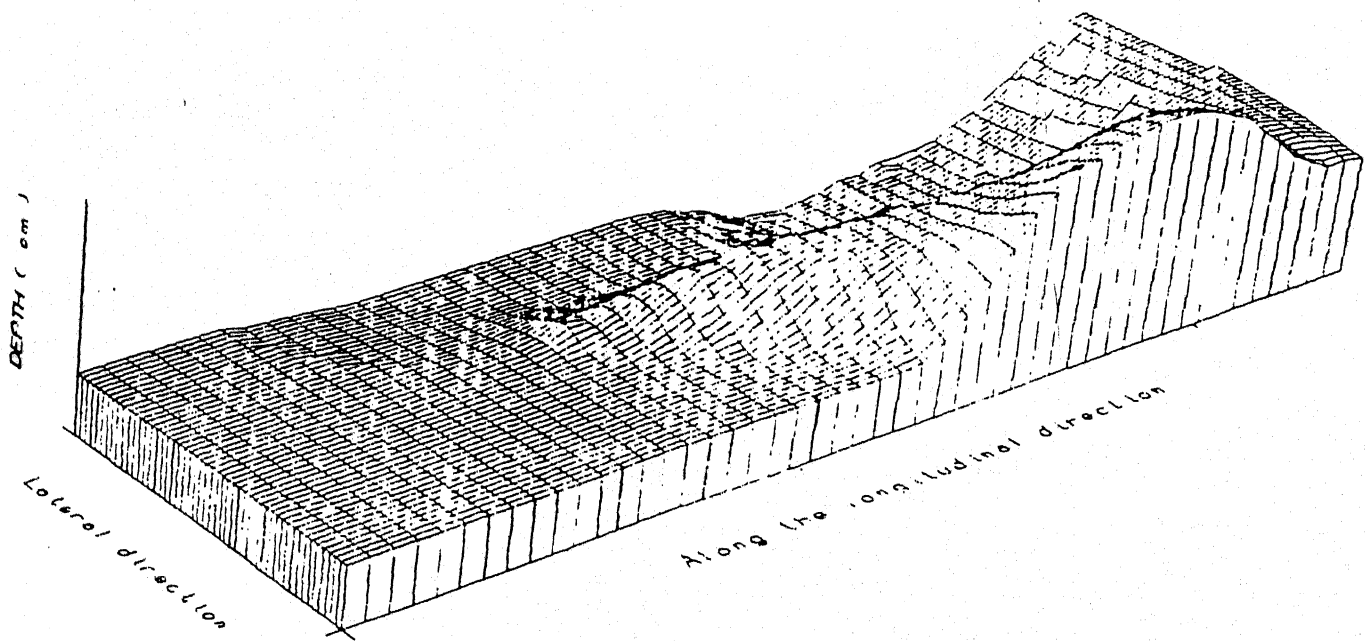
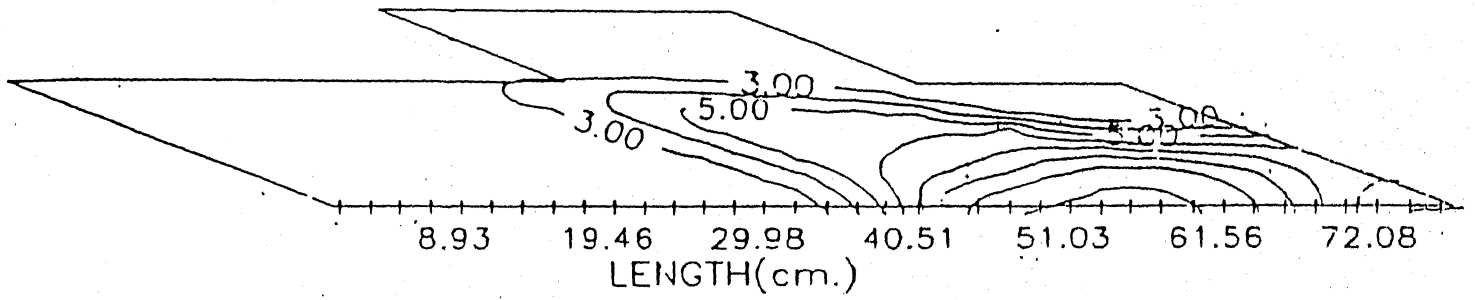
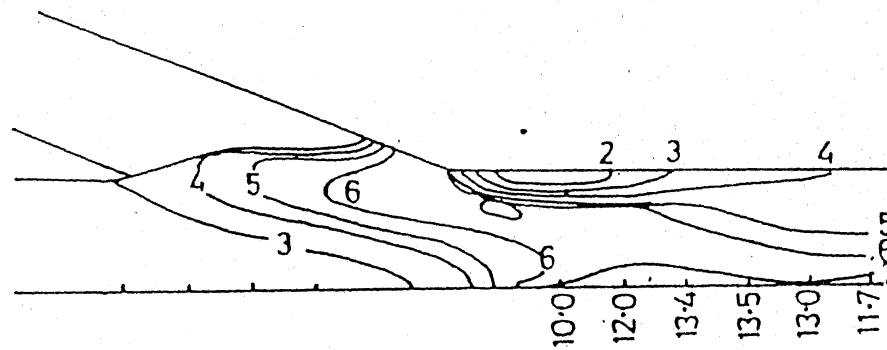


Fig.4.2 Water Surface Profile for Run 1





(a) Computed



(b) Measured

Fig.4.5 Water level Contour for Run 1

Table 4.1

Experimental details of the three selected runs

Run #	$F_u$	$F_l$	$h_u$ (cm)	$h_l$ (cm)
1	5.25	6.2	2.65	1.98
2	4.5	4.5	2.65	2.65
3	6.2	5.25	2.65	3.58

The mathematical model was run for the above test conditions using a numerical grid of  $\Delta x = \Delta y = 3.5$  cm. This corresponds to 9 nodes in the main channel. Choice of grid size was based on balancing computational speed with the desired accuracy. The computational time step,  $\Delta t$  was controlled by the courant number and grid size. As mentioned earlier the upper limit for the Courant number to achieve numerical stability required some amount of numerical experimentation. The Courant number for the runs ranged from 0.65-0.85. The dissipation coeff.  $K$ , was determined by trial and error. As discussed in chapter 3, the influence of  $K$  upon the results depends on gradients in flow depths as well as on grid size.  $K$  should be as small as possible and at the same time it should reduce the higher order numerical oscillations. The  $K$  value for the above runs was 0.9. The roughness coeff. is assumed to be zero since no information on this was

CENTRAL LIBRARY  
 Acc. No. A. 112558

TABLE 4.2 ;  $\delta = 22.5^\circ$ 

#	$h_u$	$h_l$	$F_u$	$F_l$	$h_a$	$h_n$	$h_e$
1	2.65	2.65	4.26	4.18	8.84	9.5	14.3
2	2.68	2.68	4.61	4.47	9.66	10.2	16.0
3	2.67	2.67	5.29	5.30	11.3	11.6	19.8
4	2.65	1.76	3.94	4.72	7.58	7.89	9.9
5	2.65	1.77	4.37	5.23	8.41	7.88	11.2
6	2.65	1.78	4.80	5.72	9.23	8.56	11.9
7	2.65	1.78	5.22	6.22	10.0	9.33	13.6
8	2.71	1.33	3.78	5.48	7.13	7.0	8.5
9	2.72	1.33	4.65	6.53	8.62	7.5	9.9
10	2.72	1.34	5.15	7.17	9.50	8.25	11.3
11	2.74	0.67	5.07	10.1	8.07	7.0	6.7
12	1.85	2.55	3.78	3.12	5.71	7.43	9.2
13	1.85	2.60	4.15	3.60	6.45	8.30	11.1
14	1.87	2.53	5.09	4.37	8.0	9.44	13.2
15	1.32	2.68	6.78	4.70	8.34	10.2	14.7
16	0.65	2.68	9.22	4.52	6.68	9.79	15.4
17	0.35	2.54	14.8	5.42	7.2	11.2	18.4
18	0.35	0.34	15.1	15.1	4.86	6.80	8.1
19	0.75	0.37	6.05	8.78	3.13	3.2	3.8
20	0.75	0.37	9.14	13.1	4.79	6.8	6.2
21	0.73	0.73	4.76	4.76	2.72	2.85	3.7
22	0.73	0.73	7.18	7.18	4.27	4.77	5.6
23	0.72	0.72	9.67	9.67	5.9	7.76	10.2
24	0.32	1.31	10.5	5.1	3.87	5.39	6.6

$h$  = maxm. flow depth

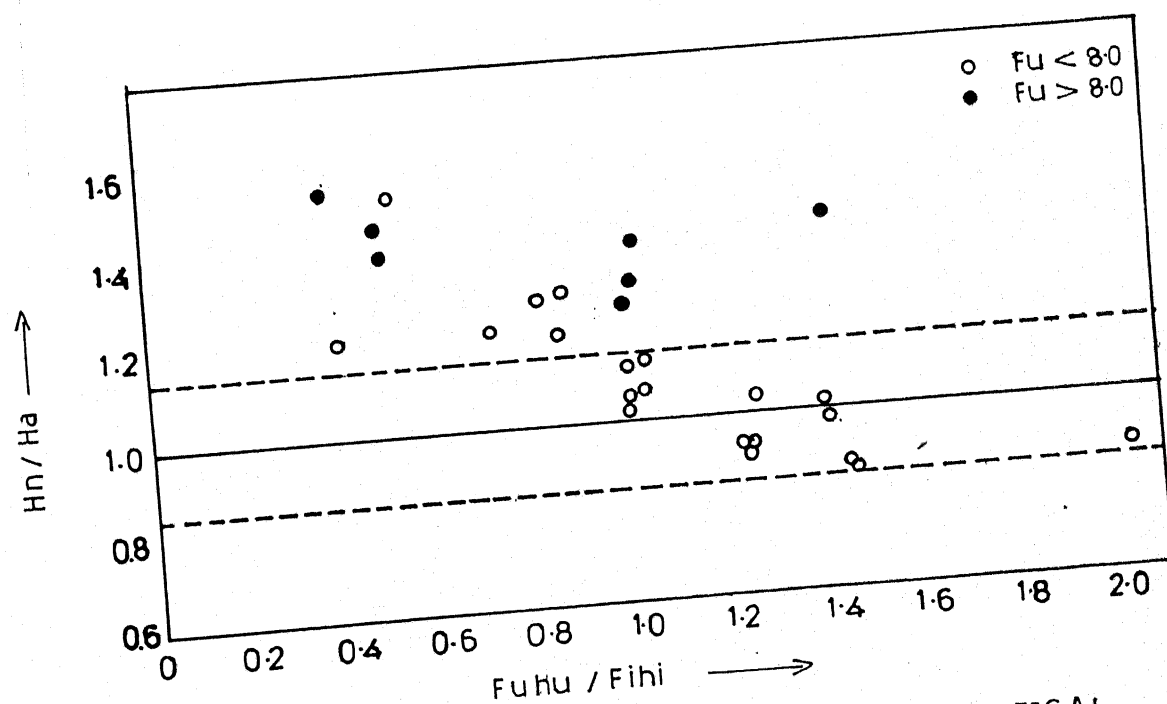
Subscripts a, n, e denotes analytical, numerical  
and experimental respectively.

TABLE 4.3 ;  $\delta = 45.0^\circ$

#	$h_u$	$h_l$	$F_u$	$F_l$	$h_a$	$h_n$	$h_e$
1	1.24	1.28	4.64	4.37	7.33	9.6	9.2
2	1.25	1.29	5.80	5.45	9.96	13.6	12.3
3	1.28	1.32	6.72	6.05	12.2	17.2	15.6
4	2.48	2.50	4.08	3.92	12.3	16.9	15.7
5	2.46	2.52	4.48	4.32	13.9	18.7	17.4
6	1.83	2.46	4.96	4.17	12.4	17.3	15.1
7	1.79	2.53	5.54	4.58	14.2	19.9	17.2
8	1.22	2.46	6.30	4.52	12.3	17.4	14.7
9	1.23	2.47	7.00	4.82	14.2	19.9	18.4
10	2.43	1.85	3.79	4.34	10.5	13.9	12.9
11	2.46	1.85	4.28	4.81	12.5	16.4	15.6
12	2.47	1.84	4.71	5.25	14.2	18.4	18.4
13	2.51	1.30	3.79	5.10	10.2	12.7	12.9
14	2.48	1.28	4.42	5.93	12.2	15.7	15.0
15	2.47	1.30	4.94	6.55	14.1	18.6	18.0
16	2.45	0.68	3.30	6.58	7.7	9.64	08.6
17	2.48	0.70	3.89	6.98	9.2	11.6	10.0
18	0.70	0.75	5.53	5.16	5.30	6.90	7.7
19	0.71	0.76	8.11	7.40	8.89	15.0	13.0
20	0.46	0.50	5.41	4.74	3.32	4.27	4.5
21	0.47	0.51	6.70	6.12	4.59	6.64	6.2
22	0.49	0.53	7.07	6.53	5.16	7.27	7.6
23	0.51	0.56	7.15	6.53	5.46	7.25	8.5

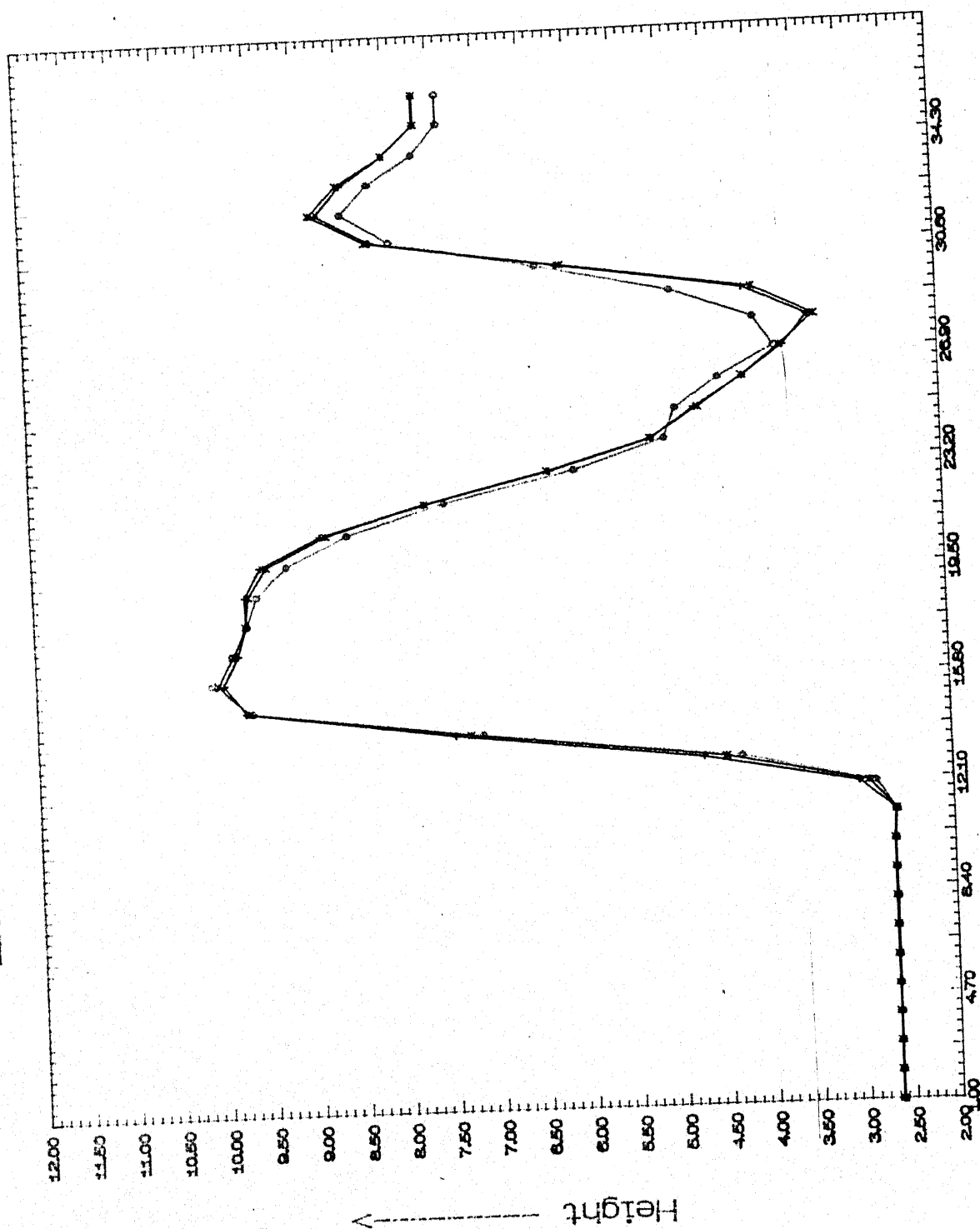
$h$  = maxm. flow depth

Subscripts a, n, e denotes analytical, numerical and experimental respectively.



A.19 DIFFERENCE IN NUMERICAL AND ANALYTICAL  
RESULTS  $\delta = 22.5^\circ$

# Effect of Courant no.



Distance along main flow →

FIG. 4.14 • = 0.65; + = 0.75; X = 0.85

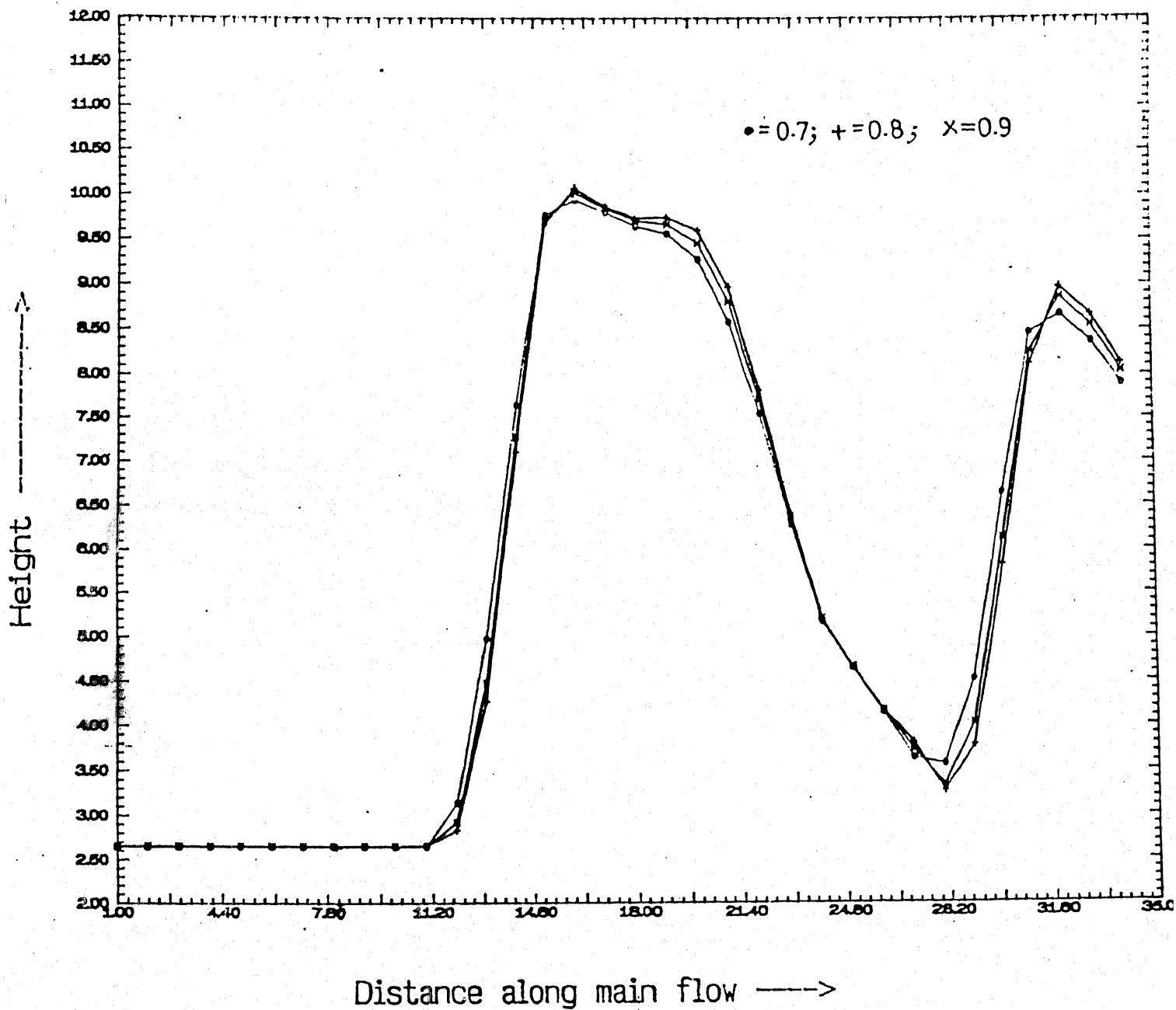


Fig.415 Effect of Variation of Dissipation Coeff.

## REFERENCES

**Abett, M.**, (1971), Boundary Conditions in Computational Procedures for Inviscid, Supersonic Steady Flow Field Calculations, Aerotherm Report 71-41.

**Abbot, M. B.**, (1975), "Weak Solutions of the Equations of Open channel Flow," in Unsteady flow in Open Channels, Mahmood, K. and Yevjevich, V., (eds), Water Resources Publications, chapter 7, pp. 283-311.

**Abbott, M. B.**, (1979) Computational Hydraulics; Elements of the Theory of Free Surface Flow, Pitman Publishing Limited, London.

**Bagge, G. and Herbich, J. B.**, (1967), "Transitions in Supercritical Open-Channel Flow," Jour. Hydr. Div., Ame. Soc. Civ. Engrs.

**Ballamudi, B. S., and Chaudhary, M. H.**, "Computation of Flow in Open Channel Transition"

**Boussinesq, J. V.**, (1872), Theory of Waves and Surges which Propagate the Length of a Horizontal Rectangular canal, Imparting to the fluid contained within the Canal Velocities that are Sensibly the Same from Top to Bottom, Jour. Math. Pures Appliquees.

**Cunge, J. A., Holly, F. M. and Verwey, A.**, (1980), Practical Aspects of Computational River Hydraulics, Pitman Publishing Limited, London.

**Cunge, J. A.**, (1975), "Rapidly Varying Flow in Power and Pumping Canals," in Unsteady Flow in Open Channels, Mahmood, K. and Yevjevich, V. (eds), Water Resources Publications.

**Chaudhary, M. H.**, (1987), Applied Hydraulic Transients Sec. Ed., Van Nostrand Reinhold Company, New York.



**Dakshinamoorthy, S.**, (1977), "High Velocity Flow Through Expansion," 17<sup>th</sup> Congress IAHR, Baden-Baden.

**Demuren, A. O.**, (1982), "Numerical Computation of Supercritical and Subcritical Flows in Open Channels with Varying Cross-Sections," Prac. 4<sup>th</sup> Int. Conf. Finite Elements in Water Resources, K.P. Holz (ed.), Hannover, Germany.

**Fennema, R., and Chaudhary, M. H.**, (1987), "Simulation of One-Dimensional Dam Break Flows," Jour. of Hydr. Research.

**Flokstra, C.**, (1977) , "The Closure Problem for depth averaged Two-Dimensional Flow," 17<sup>th</sup> Congress IAHR, Baden-Baden.

**Garcia, R. and Kahawita, R. A.**, (1986), "Numerical Solution of the St. Venant Equations with the MacCormack Finite Difference Scheme," Int. Jour. Numer. Meth. in Fluids.

**Gharangik, A. M.**, (1988), Numerical Simulation of Hydraulic Jump, paper under preparation for review in the publication, Journal of the Hydraulic Engineering, ASCE.

**Hager, W.** (1989) Supercritical flow in open Channel Junctions, Journal of the Hydraulic Engineering, ASCE. Vol.115 No.5.

**Hager, W. and Bretz, N.** (1987), discussion of "simplified Design of Contractions in Supercritical Flow," by Sturm, T., Jour. of Hydr. Engr., Amer. Soc. Civ. Engrs., vol. 113, no. 3, March, pp 422-424.

**Herbich, J. B. and Walsh, P.**, (1972), "Supercritical Flow in Rectangular Expansions," Jour. Hydr. Div., Amer. Soc. Civ. Engrs., vol. 98, no.9, Sept., pp 1691-1700.

**Ippen, A.T. and Harleman, D.R.F.**, (1950). Studies on the validity of the Hydraulic analogy to Supercritical flow: Parts 1 and 2, USAF Technical report No. 5985.

**Ippen, A.T. and Harleman, D.R.F., (1956).** "Verification of Theory for Oblique Standing Waves," Trans. Amer. Soc. Civ. Engr., Vol. 21, pp 678-694.

**Ippen, A.T. et. al., (1951),** Proceedings of a Symposium on High-Velocity Flow in Open Channels, Trans. Amer. Soc. Civ. Engrs., vol. 116, pp. 265-400.

**Ippen, A.T. and Knapp, R.T., (1936),** "A study of the high velocity flow in Curved Channels of Rectangular Cross section," Trans Amer. Geophysical Union, 17<sup>th</sup> Annual meeting, pp. 516 -521.

**Ippen, A.T. and Knapp, R.T., (1938),** "Curvilinear flow of liquids with free Surfaces at Velocities Above that of Wave Propagation," Proceedings, 5<sup>th</sup> Int.Cong. of Applied Mechanics, Cambridge, Massachusetts, pp.531.

**Ippen, A.T. and Dawson, J. H., (1951),** "Design of Channel Contractions," Symposium on High-Velocity flow in Open Channels, Trans. Amer. Soc. Civ. Engrs., vol. 116, pp. 326-346.

**Ippen, A.T. and Harleman, D. R. F., (1950),** Studies on the Validity of the Hydraulic Analogy to Supersonic Flow: Part 1 and Part 2, USAF Technical Report No. 5985, May.

**Jimenez, O.F. (1987).** "Computation of Supercritical Flows in Open Channels," thesis submitted for the degree of Master of Science, Washington State University.

**Jimenez, O.F. and Chaudhary, M.H., (1988).** "Computation of Supercritical Free Surface Flow," Jour. of Hydr. Eng., Amer. Soc.Civ.Engr., Vol.114, No.4, Apr., pp.377-395.

**Jameson, A., Schmidt, W., and Turkel, (1981),** Numerical solutions of the Euler equations by Finite Volume method using Ranga-Kutta Time-Stepping Scheme, AIAA 14<sup>th</sup> Fluid And Plasma Dynamics conference, Palo Alto, California, AIAA 81-1259.

**Knapp, R. T., (1951),** "Design of Channel Curves for

supercritical flow," Symposium of High- Velocity flow in Open Channels, Trans. Amer. Soc. Civ. Engrs., vol. 116, pp. 296-325.

**Katopodes, N.,** (1984b), "Two-Dimensional Surges and Shocks in Open Channels," Jour. Hydr. Div., Amer. Soc. Civ. Engrs., vol. 110, no. 6, June, pp. 794-812.

**Kroll, N. and Jain, R. K.,** (1987). Solutions of Two-dimensional Euler Equations-experience with a finite Volume Code, DFVLR-FB87-41, DFVLR, Institute für Entwurfsaerodynamik, Braunschweig.

**Laitone, E. V.,** (1952), "A study of Transonic Gas Dynamics by the Hydraulic Analogy," Jour. Aeronautical Sciences, vol. 19, no. 4, April, pp. 265-272.

**Lai, C.,** (1986), "Numerical Modelling of Unsteady Open Channel flow," in Advances in Hydrosience, Yen, B. C. (ed.), vol. 14, Academic Press, pp. 162-333.

**Lax, P., and Wendroff, B.,** (1960), "System of conservation laws," Commun. Pure and Applied Math., vol. XIII, pp. 217-237.

**Moretti, G.,** (1982), "Experience on Initial and Boundary Conditions," in Numerical Aspects of Aerodynamics flows, Cebeci, T. (ed.), Springer-Verlag, pp. 15-34.

**Preiswerk, E.,** (1940), Application of the Methods of Gas Dynamics to Water Flows with Free Surface, Technical Memoranda Nos. 934-935, National Advisory Committee for Aeronautics.

**Pandolfi, M.,** (1972). "Numerical Experiments on Free Surface Water Motion with Bores," Proc. 4<sup>th</sup> int. Conf. on Numerical Methods in fluid Dynamics, Lecture Notes in Physics No. 35, Springer-Verlag, pp. 304-312.

**Rouse, H.,** (1938), Fluid Mechanics for Hydraulic Engineers, MacGraw-Hill Book Co., New York.

**Rastogi, A. K. and Rodi, w.,** (1978), "Predictions of Heat and Mass Transfer in Open Channels," Jour. Hydr. Engr., Amer. Soc. Civ. Engrs., vol. 104, no. 3, March, pp. 397-419.

**Sturm, T.**, (1985), "Simplified Design of contraction in Supercritical flow," jour. Hydr. Engr., Amer. Soc. Civ. Engrs. vol. 96, no. 12, pp. 2581-2610.

**Stoker, J. J.**, (1957). Water Waves, Interscience Publisher, New York.

**Villegas, F.**, (1976), "Design of the Punchina Spillway," Water Power and Dam Construction, Nov., pp. 32-34.